



Coherent Rayleigh scattering in the high intensity regime

Mikhail N. Shneider ^{a,*}, P.F. Barker ^b, Xingguo Pan ^a, Richard B. Miles ^a

^a Department of Mechanical and Aerospace Engineering, Princeton University, Princeton, NJ 08544, USA

^b Department of Physics, School of Engineering and Physical Sciences, Heriot-Watt University, Edinburgh EH144AS, UK

Received 29 January 2004; received in revised form 7 May 2004; accepted 10 May 2004

Abstract

Coherent Rayleigh scattering (CRS) is studied in the high intensity regime, where the optical lattice potential approaches the thermal energy of the gas particles. We describe this optical-kinetic process using a 1-D Boltzmann equation with an arbitrary strong optical force and show that in this regime a line shape narrowing phenomenon is predicted and that the signal intensity saturates when complete trapping of particles is reached. We discuss the impact of these processes on the application of coherent Rayleigh scattering as a gas phase diagnostic tool.

© 2004 Elsevier B.V. All rights reserved.

PACS: 33.20.Fb; 42.50.Vk; 42.65.Hw; 51.10.+y

Keywords: Coherent Rayleigh scattering; Line shape; Optical lattice

Coherent Rayleigh scattering (CRS) [1] and coherent Rayleigh–Brillouin scattering (CRBS) [2] are recently developed non-resonant, non-linear, gas phase diagnostic tools which have been used to provide useful gas kinetic information over a wide range of temperatures and densities. In CRBS, two pump laser beams are used to form a periodic potential, often called an optical lattice. Optical lattices have been widely used to trap,

transport, and even cool ultra cold gases [3,4]. In CRS and CRBS an optical lattice is used to generate a gas density perturbation in ‘hot’ gases via the electrostrictive force. The signal is formed by scattering a probe beam from the induced density wave and the resultant line shape of the scattered light is given by the power spectrum of the gas density perturbation waves, which in turn are determined by optical excitation and the concomitant collisional relaxation. Both of these techniques are attractive because they are characterized by a straightforward line shape analysis which can be used to extract gas temperature, density and viscosity. Coherent Rayleigh scattering is

* Corresponding author. Tel.: +1-609-2581-022; fax: +1-609-2581-139.

E-mail address: shneyder@princeton.edu (M.N. Shneider).

a limiting case of CRBS, and describes an ideal collisionless system which is valid when the mean free path $l_c \gg \lambda_1$, where

$$l_c = \frac{1}{\sqrt{2\pi d^2 N}} = \frac{k_b T}{\sqrt{2\pi d^2 p}},$$

d is the diameter of the molecule, N is the density of the molecules and p is the pressure, λ_1 is the period of the optical lattice used to create the perturbation. To date, the development of CRBS and CRS has focused on the so called low intensity regime, where the applied optical potential is much smaller than the mean kinetic energy of the gas. In this regime the electrostrictive force induced by the interaction between the optical potential and the polarizability of the particle induces a weak periodic density perturbation in the velocity distribution function. At low densities, when the collisionless approach is valid, representative of pressures $p \ll k_b T / \lambda_1 \sqrt{2\pi d^2}$, it is often desirable to increase the density modulation by increasing the amplitude of the periodic potential. However, when much larger optical potentials are applied, the velocity distribution is significantly modified by the optical potential and the simplified perturbative analysis which has been used to date cannot be applied.

Coherent Rayleigh scattering, and its application as a diagnostic tool, has been previously studied [1,5]. In these works the optical lattice well depths were negligibly small in comparison with the thermal energy of the gas, and the line shape of the CRS signal did not depend on the laser intensity. In this paper, we describe coherent Rayleigh scattering in a different regime, where the velocity distribution function of the gas is more strongly perturbed using deeper optical potentials produced by higher intensity pump fields. This regime is characterized by optical potentials that are greater than $\sim 0.1 k_b T$. In this regime we describe a new saturation and line shape narrowing phenomena, and study this as a function of pump intensity. Finally, we describe how this behaviour impacts on the application of CRS as a gas phase diagnostic.

In previous studies, perturbative methods have been used to predict the power spectrum of the gas density waves induced by periodic optical potentials, often called lattices. This type of analysis

can be used when the pump intensity is weak, as the gas particles' energy distribution function is only slightly perturbed by the optical potential. In this regime, a linearized forcing term within the 1-D Boltzmann equation can be employed to model the evolution of velocity distribution function in space and time. It has been successfully used to model measured line shapes in CRS and CRBS experiments in atomic and molecular gases [1,2]. The criterion for linearizing the force term can be examined by considering an optical lattice generated by two single mode laser beams of equal intensity with electric field amplitude, E_0 . The angular frequency difference between each beam is ω . The periodic potential energy well associated with this optical lattice has a maximum depth of

$$U_0 = \frac{1}{2} \alpha E_0^2, \quad (1)$$

where α is the polarizability of the gas particle of interest.

When the potential well depth is much less than the characteristic temperature ($U_0 \ll k_b T$), the perturbation induced by the lattice is negligible as shown previously [1,2]. For the case, where $U_0 \sim 0.1 k_b T$, many atomic and molecular species can be trapped by the lattice potential and the velocity distribution function is no longer a 1-D Maxwell–Boltzmann distribution along the lattice direction. In this regime the linearization of the force term is no longer appropriate. For a gas at room temperature, $k_b T \sim 4.1 \times 10^{-21}$ J, and for argon with static polarizability of $\alpha = 1.805 \times 10^{-40}$ Cm²/V an intensity of 6×10^{16} W/m² is required to produce a comparable optical potential.

Gas particles that move at, or near, the phase velocity of the optical lattice are trapped by the potential and form the periodic perturbation from which the probe beam scatters. If the frequency difference of the two pump beams is varied, the amplitude of the gas density perturbation changes and this variation is observed in the measured line shape in a CRS experiment. In such an experiment, a single mode probe beam of fixed frequency is scattered from the periodic density modulation created by two single frequency pump beams, one of which is fixed in frequency while the other is scanned. The theoretical model presented in [1]

assumed that the coherent Rayleigh scattered line shape is given by the intensity of the scattered light as a function of the frequency difference between two single mode pump beams.

Following [1], we use a one dimensional kinetic equation to study the gas density perturbation generated by the optical lattice.

$$\frac{\partial f}{\partial t} + v \frac{\partial f}{\partial z} + a \frac{\partial f}{\partial v} = \left[\frac{\delta f}{\delta t} \right]_{\text{collision}}, \quad (2)$$

where $f=f(z,v,t)$ is the energy distribution function as a function of space z , velocity v , and time t , and $a(z,t)=F(z,t)/M$ is the acceleration of a gas particle of mass M due to the optical dipole force $F(z,t)$. We separate the distribution function into two parts so that

$$f(z, v, t) = f_0(v) + f_1(z, v, t), \quad (3)$$

where the equilibrium distribution function is given by

$$f_0(v) = \frac{1}{\sqrt{\pi}v_0} \exp\left(-\frac{v^2}{v_0^2}\right), \quad (4)$$

and $f_1(z, v, t)$ is the deviation from the equilibrium distribution caused by the optical dipole force field. Here $v_0 = \sqrt{2k_b T/M}$, and T is the gas temperature and M the mass of the particles.

Ideally, there are no collisions between the gas particles in coherent Rayleigh scattering, therefore, the collision term can be neglected and $\left[\frac{\delta f}{\delta t}\right]_{\text{collision}} = 0$. A numerical solution for $f(z, v, t)$ is sought for dilute gases using a simple collision model $\left[\frac{\delta f}{\delta t}\right]_{\text{collision}} = -v_c(f - f_0) = -v_c f_1$, where v_c is the collision frequency. As discussed in [6], this collision model only conserves mass, and is not appropriate for modeling highly collisional gases. When collisions are rare, however, this approximation is acceptable even if the distribution function deviation, f_1 , is significant.

We rewrite Eq. (2) for f_1 as

$$\frac{\partial f_1}{\partial t} + v \frac{\partial f_1}{\partial z} + a \frac{\partial}{\partial v} (f_0 + f_1) = -v_c f_1. \quad (5)$$

The distribution function deviation $f_1(z, v, t)$ may be solved numerically from Eq. (5). This is a typical hyperbolic equation, and we solve it by a finite difference method of second order accuracy. Two algorithms, the Lax–Wendroff [7] and the Mac-

Cormack methods [8] were used and yield identical results.

The acceleration induced by the optical lattice is given by

$$a(z, t) = \frac{1}{2} \frac{\alpha k}{M} E_0^2 \cos(kz - \omega t) [1 - \exp(-t/\tau_F)],$$

where the exponential factor indicates the rise time τ_F of the lattice fields. In the following calculations, we set $\tau_F=1$ ns with initial condition $f_1(z, v, t=0)=0$. The boundary conditions are given by $f_1(z, v=-\infty, t)=0$, $f_1(z, v=+\infty, t)=0$, and $f_1(z_0+\lambda_l, v, t)=f_1(z_0, v, t)$, where λ_l is the wavelength of the optical lattice. We consider pump beams of two counter propagating optical fields that could be, for example, produced by the frequency doubled output from two frequency doubled Nd:YAG lasers creating $\lambda_l=532/2=266$ nm. We consider 532 nm light because the second harmonic of the laser is usually available, and additionally in an experiment the visible 532 nm radiation simplifies alignment. Any wavelength can in principle be used for CRS, but the scattering cross-section decreases with increasing wavelength to the fourth power. To solve Eq. (5), both the space and velocity grids need to satisfy the Courant condition and in addition, the velocity grid needs to be small enough so that the potential well over one period is sufficiently resolved.

The square of the gas density perturbation, as measured by a coherent Rayleigh scattering experiment is

$$\langle \delta n_\omega^2 \rangle = \frac{n_0^2}{\lambda_l} \int_0^{\lambda_l} \left(\int_{-\infty}^{+\infty} f_1(v, z, t) dv \right)^2 dz,$$

but alternative definitions may be given by averaging over time for one oscillation period and identical results would be obtained. The numerical calculation shown in Fig. 1 is time accurate and shows the evolution of the perturbation. This calculation was performed for argon at pressure $p=5$ kPa, a temperature of $T=273$ K, and the pump beams crossed at an angle 178° .

Fig. 1 shows the development of the density perturbation with time when the pump beam amplitude is ($E_0=5.0 \times 10^7$ V/m, $U_0=16$ mK). The frequency difference between the two pump beams of 0.5 GHz corresponds to a optical lattice phase

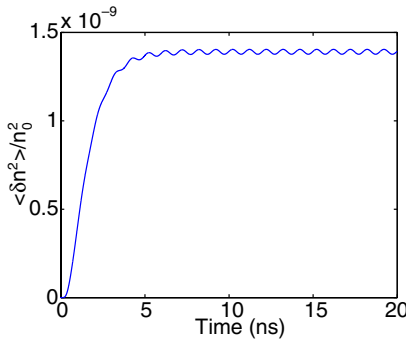


Fig. 1. Density perturbation generated by a pulsed optical lattice with frequency difference between the two pump beams of 0.5 GHz. The electric field amplitude of the each beam is 5.0×10^7 V/m.

velocity of 133 m/s. In the figure the density perturbation rises to a steady state value of $\langle \delta n^2 \rangle / n_0^2 = 1.4 \times 10^{-9}$ after 5 ns. The solution yields the same results as the linear model [1].

Next, we consider the case for pump beams with an electric field $E_0 = 5.0 \times 10^8$ V/m (intensity of 3.3×10^{14} W/m²) corresponding to an optical potential of 1.6 K. This intensity is lower than the breakdown threshold for the argon gas at the given conditions [9]. The density perturbation is much stronger as shown in Fig. 2 for $\Delta\omega/2\pi = 0.5$ GHz with a density perturbation of $\langle \delta n^2 \rangle / n_0^2 = 1.19 \times 10^{-5}$. In the low intensity regime the signal scales as $\langle \delta n^2 \rangle$ therefore the CRS signal for this intensity would be four orders

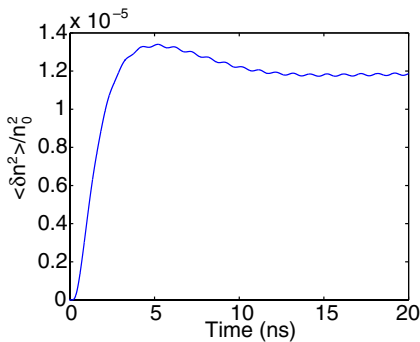


Fig. 2. Density perturbation generated by an optical lattice with frequency difference between the two pump beams of 0.5 GHz. The electric field amplitude of the each beam is 5.0×10^8 V/m.

of magnitude larger than for the $E_0 = 5.0 \times 10^7$ V/m case.

The calculated line shape of the coherent Rayleigh scattered light, as a function of the frequency difference between the fields, is shown in Fig. 3. To calculate these values, the steady state value of the density perturbation was used. The low intensity pumps yields the same line shape predicted by the linearized model as expected. This can be seen from Fig. 4 by comparing the coherent Rayleigh scattering profiles for $E_0 = 4.8 \times 10^8$ V/m and $E_0 = 5.0 \times 10^8$ V/m curves calculated using the numerical scheme that includes the non-linear term as discussed above. As E_0 increases by 4%, the density perturbation increases more significantly at line center.

One may suppress the non-linear term in the calculation to obtain a linearized numerical solution of the density perturbation which can be seen in Fig. 4 for the same high intensity field $E_0 = 5.0 \times 10^8$ V/m, the linearized perturbation would be stronger than the non-linear case but there is no narrowing.

At a given gas temperature, the spontaneous Rayleigh scattering spectral profile reflects the Doppler shift imparted to the scattered light by the 1-D Maxwell–Boltzmann velocity distribution function of a gas in thermal equilibrium. For

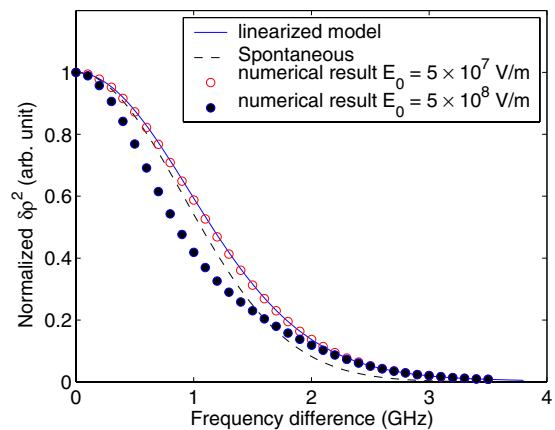


Fig. 3. The coherent Rayleigh scattering line shape for different pump beam intensity. The circles are numerical results of the non-linear model. The curves are normalized to unity at zero frequency difference. Also indicated is the spontaneous Rayleigh scattering line shape.

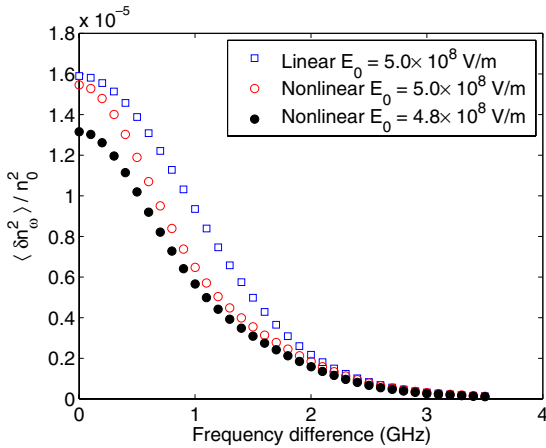


Fig. 4. Numerical results of coherent Rayleigh scattering line shapes for different pump beam intensities. The narrowing of CRS profile at higher intensities is shown as well as the wider line shape obtained from the linearized model.

CRS, in the linearized regime, one would intuitively expect that the scattered line shape to be narrower than the spontaneous case because it is a non-linear scattering process which scales as the square of the density perturbation. However, the CRS line shape is broader in this regime because untrapped species that are not travelling at the lattice velocity, but whose velocity is still modified by it, contribute strongly to the total perturbation and therefore to the spectral profile of the CRS signal.

Hence, the wings of the CRS line shape are wider because there is a significant contribution from the untrapped species at the center of the initial distribution function that those that are trapped by the lattice velocity in the wings of the original distribution [1].

As we have shown for intense pumping ($E_0 = 5.0 \times 10^8$ V/m), the CRS line shape becomes significantly narrower than both the low intensity coherent case and also to the spontaneous Rayleigh scattering. Narrowing in this regime occurs because at these intensities more of total perturbation is due to species trapped by the lattice than due to the untrapped fraction whose velocity is modified but not trapped by the lattice potential. A comparison between the perturbation to the original Boltzmann distribution function in the two regimes in Fig. 3 illustrates this process. Each graph shows the perturbation for a lattice velocity of 381 m/s produced by a potential of 0.0159 K ($E_0 = 5.0 \times 10^7$ V/m; Fig. 5(a)) and 1.59 K ($E_0 = 5.0 \times 10^8$ V/m; Fig. 5(b)), respectively. The velocity spread of $2\Delta v = \sqrt{8U_0/M}$ of particles trapped by the potential is also shown by the dotted square indicating the relative fraction of the perturbation due to the trapped and untrapped components. The smaller trapped fraction and the correspondingly wider velocity spread of the low intensity case, when compared to the high intensity perturbations, indicates why the CRS signal which

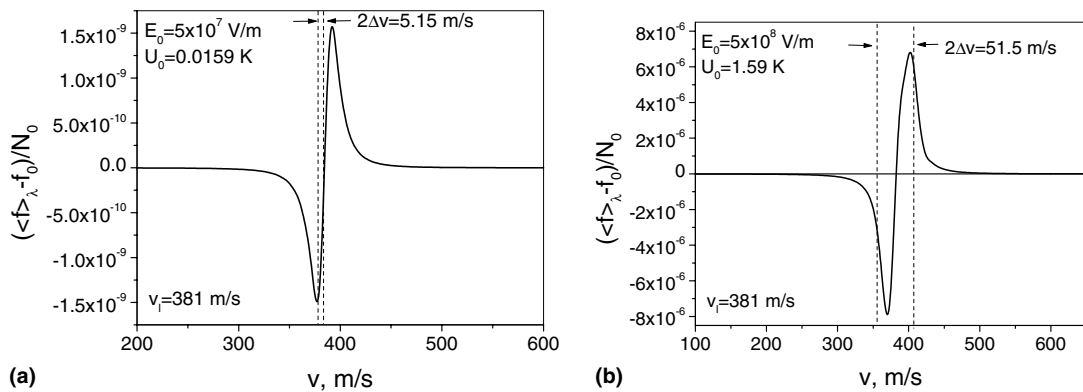


Fig. 5. Graphs of the induced perturbation for a lattice velocity of 381 m/s produced by a potential of: (a) 0.0159 K ($E = 5.8 \times 10^7$ V/m) and (b) 1.59 K ($E = 5.8 \times 10^8$ V/m) corresponding to the two CRS profiles in Fig. 3. The trapped fraction enclosed by the dotted lines in each graph is a smaller fraction of the perturbed velocity distribution function. However, the trapped fraction is larger for the smaller field and indicates why the line shape in Fig. 3 is wider for the higher field case.

scales as the square of the density perturbation given by $\delta\rho = \frac{1}{N} \int_{-\infty}^{\infty} \delta f dv$, is wider for the low intensity case. In contrast, for the higher intensity case most of the perturbed distribution is due to trapped species because a larger fraction of the perturbation is localized around velocity spread $2\Delta v$ determined by the well depth.

Of importance for the application of CRS for gas phase diagnostics is how the signal intensity scales with pump intensity. Since the line shape changes in the high intensity regime it is natural to expect that the CRS would change from an I^2 dependence as a function of pump intensity expected in the low intensity regime. To study this we have plotted signal intensity, which is proportional $\langle(\delta n)^2\rangle/n_0^2$, as a function of pump beam intensity up to 1×10^{17} W/m². We have not considered intensities fields higher than this because either tunneling or multiphoton ionization will become important above these intensities [10]. The graph of CRS signal intensity as a function of pump intensity is shown in Fig. 6 on a logarithmic plot. Also plotted is the expected I^2 pump intensity dependence at low intensities. At intensities below 10^{13} W/m², the CRS signal has an I^2 dependence with pump intensity. Above this inten-

sity the CRS intensity dependence flattens as the more of the species are trapped within the lattice. If higher intensities could be used to produce well depths comparable to the gas temperature (i.e., 297 K), and that no ionization or dissociation occurred, the dependence with pump power should limit to I^0 dependence since essentially all species would be trapped. This saturating behaviour will be more obvious at lower gas temperatures as the momentum spread of the gas is narrowed. Therefore, for diagnostic applications at lower temperatures, we cannot assume a I^2 dependence even below the 10^{13} W/m² value obtained for the 273 K case shown in Fig. 6. From the results presented, we can expect narrowing of the CRS signal when the optical potential depth becomes of order of 1% of the gas molecules thermal energy and, therefore, at gas temperature ~ 5 K we can expect observable narrowing at $I = 10^{13}$ W/m².

In this paper, we have studied the effect of optical lattice well depth on coherent Rayleigh scattering signals when the potential well depth approaches the gas temperature. We have found that the power spectrum of the density perturbation, and therefore the line shape of the CRS signal, changes significantly with the pump beam intensity in this high intensity regime. For an argon gas at 273 K an I^2 dependence with pump intensity is expected up to 10^9 W/cm² but increases at a lower rate at higher intensities. The process is attributed to the finite extent to which modulation of the gas density by the lattice beams can occur due to the finite reservoir of gas particles. The line narrowing feature observed in the CRS spectra is not predicted by the linearized model, and additionally, is even narrower than the spontaneous Rayleigh scattering line shape. We note that this is a new line narrowing phenomena that only occurs in CRS. We note that it is not a type of Dicke narrowing [11,12], although we would expect Dicke narrowing of spontaneously scattered light from particles trapped in the lattice at these pump powers. The scattered light that forms the CRS line shape results from scanning the lattice velocity across the velocity distribution profile. Therefore, at any one lattice velocity, the signal is due to the integrated scattered light from all of the trapped particles and therefore we do not see

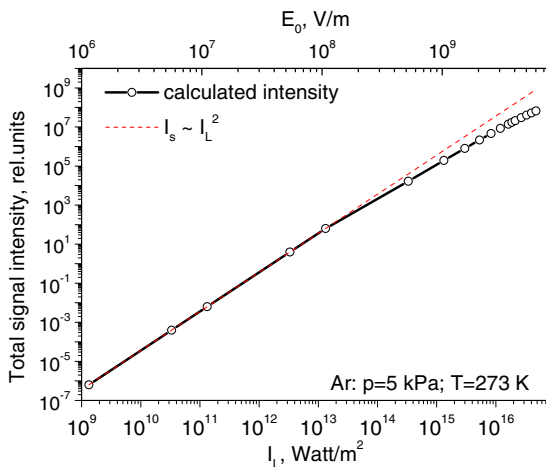


Fig. 6. Dependence on coherent Rayleigh scattering with pump intensity. At low intensities the CRS signal scales as the square of the pump beam intensity while in high intensity regime it is less and begins to saturate due to the finite reservoir of particles available to take part in the scattering process.

Dicke narrowing. Importantly, we emphasise that when using coherent Rayleigh scattering line shape as a laser diagnostic technique for temperature, one needs to consider the effect of line narrowing at high intensities, and that the simple near Gaussian analysis for the line shape cannot be used in this regime. In addition, the integrated signal, which at low intensities is proportional to the square of the density, cannot be used to determine density at high intensities *I*.

References

- [1] J.H. Grinstead, P.F. Barker, Phys. Rev. Lett. 85 (2000) 1222.
- [2] X. Pan, M.N. Shneider, R.B. Miles, Phys. Rev. Lett. 89 (2002) 183001.
- [3] D.R. Meacher, Contemp. Phys. 39 (1998) 329.
- [4] L. Guidoni, P. Verkerk, J. Opt. B: Quantum Semiclass. Opt. 1 (1999) R23.
- [5] X. Pan, P.F. Barker, A. Meschanov, J.H. Grinstead, M.N. Shneider, R.B. Miles, Opt. Lett. 27 (2002) 161.
- [6] P.L. Bhatnagar, E.P. Gross, M. Krook, Phys. Rev. 94 (1954) 511.
- [7] W.H. Press, S.A. Teukolsky, W.T. Vetterling, B.P. Flannery, Numerical Recipes in C: the Art of Scientific Computing, second ed., Cambridge University Press, New York, 1992 Chapter 19.
- [8] R.B. Horne, M.P. Freeman, J. Comput. Phys. 171 (2001) 182.
- [9] Y.P. Raizer, Gas Discharge Physics, Springer, Berlin, NY, 1991.
- [10] M.H. Mittleman, Introduction to the Theory of Laser-atom Interactions, Plenum Press, New York, 1993.
- [11] R.H. Dicke, Phys. Rev. 89 (1952) 472.
- [12] C.J. Meinrenken, W.D. Gillespie, S.O. Macheret, W.R. Lempert, R.B. Miles, J. Chem. Phys. 106 (1997) 8299.